Available online at www.eccomasproceedia.org
Eccomas Proceedia COMPDYN (2021) 4568-4581

ECCOMAS
Proceedia

COMPDYN 2021
8th ECCOMAS Thematic Conference on
Computational Methods in Structural Dynamics and Earthquake Engineering
M. Papadrakakis, M. Fragiadakis (eds.)
Streamed from Athens, Greece, 28 - 30 June 2021

SEISMIC RISK ASSESSMENT OF A PROCESS PLANT UNIT ACCOUNTING FOR DYNAMIC INTERACTION

George Karagiannakis[1,2] **and Luigi Di Sarno**[1,3]

[1] University of Sannio, Piazza Roma 21, 82100 Benevento, Italy
karagiannakis@unisannio.it, ldisarno@unisannio.it

[2] European Commission Joint Research Centre (JRC), Ispra (VA), Italy
georgios.karagiannakis@ec.europa.eu

[3] University of Liverpool, Liverpool L69 3BX, UK
luigi.di-sarno@liv.ac.uk

Abstract

Analytical fragility curves for structures used in chemical plants are not commonly derived because of the high computational cost. In contrast, empirical curves are utilized within a quantitative risk assessment framework given that they can be found easily and adopted for different structural configurations. Arguably, analytical fragility curves can account for dynamic idiosyncrasies due to the interaction of a supporting structure and equipment that diversify from one process unit to another. Additionally, the use of an efficient and sufficient earthquake intensity measure is essential for deriving robust fragility curves. Peak ground measures that are commonly adopted for risk assessment may not be efficient to describe more complex systems with higher mode effects.

Using time-efficient modelling, the present analytical study intends to evaluate the seismic risk to a hydrodesulphurization unit, a process used in modern refineries to remove sulphur from refined petroleum products. The 3D model of the unit consists of an irregular steel supporting structure, several vessels as well as a piping network. To attain a robust modelling, the effects of panel zone configuration is examined. Furthermore, the seismic response of steel structure and piping is seen through the lens of different intensity measures. In the end, the most efficient and sufficient intensity measure is considered to derive fragility functions and estimate the annual frequency of exceedance of two different limit states. The results show that the steel frame is more vulnerable than the piping due to pounding effects of a heavy vessel at high level. In addition, the results highlighted that the spectral acceleration is an efficient and sufficient intensity measure. However, the spectral acceleration should be used at different vibration periods due to higher mode effects of equipment, which cannot always be expressed as a percentage of fundamental period of the structure. Thus, the standard approach based on the average spectral acceleration, as proposed in the literature, may not apply for process units of this type.

Keywords: process unit; steel structure; pipes; seismic hazard; dynamic interaction; fragility; risk assessment

ISSN:2623-3347
Peer-review under responsibility of the organizing committee of COMPDYN 2021.
doi: 10.7712/120121.8808.18488

1 INTRODUCTION

In chemical plants, supporting structures are used to carry piping and equipment for mechanical, safety and maintenance reasons. Supporting structures can vary on purpose and configuration, but two main configurations can be described: 1) pipe racks are used to carry piping that transfers products from one process unit to another and 2) steel towers are constructed to support vessels and piping at different heights. In pipe racks, the supporting structures are quite regular and they are usually considered as cantilevers during design and assessment, because of the lack of diaphragmatic behaviour and because of the point forces of pipes at the top (Figure 1a). In steel towers, structures are more irregular, in terms of mass and stiffness, they present higher mode effects and can be high-rise to accommodate all the required equipment (Figure 1b). In both cases, however, the potential risk due to piping failure can be the reason for catastrophic cascading effects given the hazardous materials involved.

Earthquakes continue to expose European countries, particularly in the Mediterranean sea, to high risk where seismic events have triggered significant destruction over the last decades [1]. Additionally, numerous major accidents events have been triggered by the seismic hazard due to damage to piping and supporting structures, causing human losses, environmental contamination and financial losses ([2]–[4]). The life-saving issue of seismic integrity inside chemical plants was also illustrated by [5], who identified 78 Natech accidents triggered by earthquakes, involving 439 pipework components (directly or indirectly damaged).

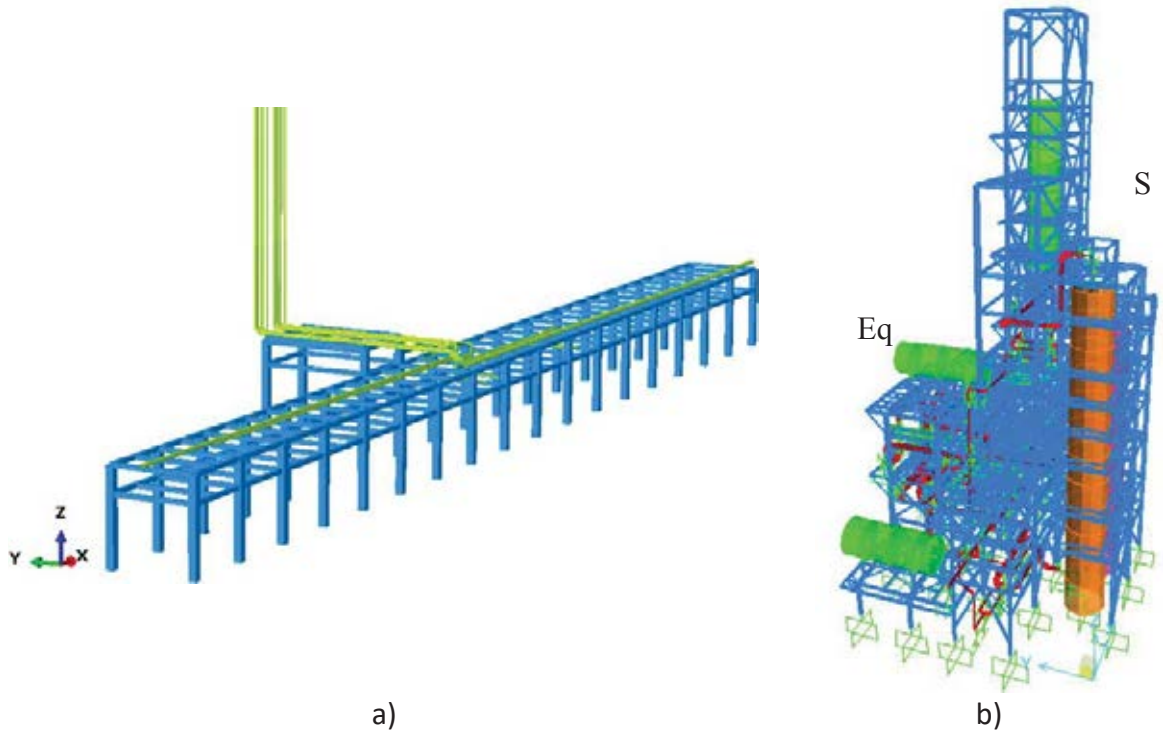

Figure 1: Different types of supporting structures inside chemical plants: a) pipe rack, b) tower with process equipment.

Seismic assessment is essential for risk reduction inside chemical plants. One of the most decisive steps of the risk assessment of major accidents triggered by seismic events is the use of fragility functions [6], which express the conditional probability of reaching or surpassing a specific damage state given an Intensity Measure (IM) of earthquake shaking. Fragility functions can be utilized prior to an earthquake within a consequence-based analysis to design strengthening measures and devise emergency response plans as well as in the aftermath of an

earthquake to prioritize inspection and determine medium- and long-term response and recovery ([7], [8]). Although the robustness of analytical fragility curves for critical process units is crucial for risk reduction inside process plants, many researchers still adopt empirical ones e.g. from HAZUS [9], because they are easily available and have applicability to different process units. Other databases e.g. SYNER-G [10] include both empirical and analytical fragility curves, though they are not exhaustive in terms of the various process units that can be found in petrochemical plants and do not account for the fragility of equipment separately. At least to the Authors' knowledge, the literature on the fragility derivation of supporting structures that account for dynamic interaction with equipment is very scarce. Even though some studies have been conducted in the past, they mainly regarded the fragility assessment at the component level and usually neglected the dynamic coupling between the supporting structures and the equipment ([11]–[14]).

Apart from modelling uncertainties, robust fragility functions should be expressed by selecting seismic IM that are representative of the seismological properties of ground motion related to site and source (sufficiency) and which reduce the record-to-record randomness (efficiency). A sufficient IM is conditionally independent of magnitude, M, and Joyner-Boore distance, Rjb; thus, these parameters have little effect on the resulting seismic demand model. Additionally, an efficient measure results in low variability of seismic demand and enables the evaluation of the demand with the least possible number of ground motions. The efficiency and sufficiency of different IMs have already been addressed for common civilian assets, bridges and transport pipelines ([15]–[18]). For example, [18] conducted a literature review on the existing fragility curves for the European building stock, and it was confirmed that typical ground measures, e.g. peak ground acceleration, velocity and displacement as well as spectral measures at the fundamental period of structures were considered efficient. When it comes to buildings with non-structural components, an average spectral acceleration based only on the fundamental period of a building was proposed by [18] and [19], so that it can be easily applied in a risk assessment procedure. However, whether this IM can be applied for high irregular and complex systems, like process units, or not is still an open question that will be discussed in the current work.

The present analytical study intends to: 1) examine the seismic response of a process unit, 2) compare the efficiency and the sufficiency of common and recently-proposed measures for which ground prediction models are easily available and which can be used within a quantitative risk assessment, and 3) estimate the seismic risk in terms of mean annual frequency of collapse for further decision making, e.g. retrofitting or response planning.

2 DERIVATION OF ANALYTICAL FRAGILITY

2.1 Methodology

Different fragility analysis methods can be adopted to derive the fragility of a structural system. The methods are generally categorized as narrow- and wide-range, depending on the range of IM values. Considering that process units are large in scale and complex, stick modelling should be used, accounting also for the analysis method with the least possible computational cost. In addition, when addressing the fragility of critical plants where high level of damage must be avoided or should occur at large seismic intensity only, it is prudent to localize the investigation of an industrial structure, at least preliminarily, at lower performance level e.g. serviceability or life safety.

To this effect, the so-called cloud analysis that belongs to narrow-range methods will be used for the present study. The probabilistic estimation of an engineering demand parameter

given an IM is attained through the least sum of the squares of the residuals method, as described in [21]. The logarithmic linear regression of seismic demand, EDP, as a function of IM is considered and described by Equation 1:

$$EDP = (a \cdot IM^b) \cdot \varepsilon$$
$$\eta_\varepsilon = 1 \; and \; \sigma_{ln\varepsilon} = \beta_{EDP|IM} \tag{1}$$

where a is an intercept and b is the slope in log-space. The lognormal random variable ε has median, η_ε, equal to unity and its logarithmic standard deviation, $\sigma_{ln\varepsilon}$, is equal to the standard deviation of the EDP for a given value of IM, $\beta_{EDP|IM}$. The latter constitutes a metric of the efficiency of the regression of tested IMs to describe the seismic response of a structure.

Assuming that the EDP follows a logarithmic standard distribution for a given IM, the logarithm of the median, $ln(\eta_{EDP|IM})$, is equal to the mean of the logarithm of EDP, $\mu_{lnEDP|IM}$. The standard deviation of the logarithm of EDP, $\sigma_{lnEDP|IM}$, is equal to the dispersion of EDP, $\beta_{lnEDP|IM}$. Therefore, the parameters of the linear regression, a and b, can be obtained by estimating the median using linear regression in the logarithmic space of "cloud" data. The cumulative lognormal distribution of the observed data is expressed by Equation 2:

$$P[EDP_D > EDP_C|IM] = \Phi\left(\frac{\ln(a \cdot IM^b) - \ln \eta_{EDP|IM}}{\beta^2_{EDP|IM}}\right)$$
$$= \Phi\left(\frac{\ln(IM) - \ln \eta_{IM|EDP}}{\beta_{IM|EDP,tot}}\right) \tag{2}$$

The total dispersion $\beta_{IM|EDP,tot}$ accounts for three types of uncertainty, namely seismic demand ($\beta_{EDP|IM}$), capacity (β_C) and limit state (β_{LS}) definition. The first type of uncertainty will be evaluated via nonlinear dynamic analyses in Section 4. The second and third uncertainty types are set equal to 0.3 and 0.4, respectively, based on common values that can be found in [9]. A more rigorous definition of the last two types of uncertainty would require a further detailed examination, which is beyond the scope of the present study. Finally, the total dispersion is evaluated by Equation 3:

$$\beta_{IM|EDP,tot} = \frac{1}{b}\sqrt{\left(\beta^2_{EDP|IM} + \beta^2_C + \beta^2_{LS}\right)} \tag{3}$$

3 CASE-STUDY

The case-study deals with the seismic assessment of an existing desulphurization process unit that is made of steel (Figure 1b). It was originally designed according to [22] for a high seismicity region. By virtue of a recent update of seismic hazard maps in the region of interest ([23]), the seismic integrity of the process unit should be assessed. The new acceleration values, S_1=1.35g and S_S=0.38g, were used for selecting seismic records consistent with the seismic hazard. The system is divided into two parts in order to facilitate the assessment in the following; in particular, the first part regards the high-rise steel structure (S) with the vertical vessel at the top (Figure 2a&b), whilst the second part is composed of a low-rise steel structure with equipment (Eq) that consists of horizontal vessels and pipes (Figure 2b). In this respect, see also Figure 1b. The system was assessed in the nonlinear regime using [24] and [25] as reference codes.

3.1 Modelling characteristics

The structural members are made of steel ASTM A36/A36M with expected yield (f_{yes}) and ultimate strength (f_{ues}) 372.32 MPa and 439.89 MPa, respectively, modulus of elasticity (E)

equal to 203 GPa, Poisson ratio (ν) equal to 0.3 and kinematic hysteretic behaviour. The lateral load resisting system is formed by ordinary braced frames in the X direction, and ordinary moment frames in the Y direction. Horizontal bracing is placed in the XY plane and some vertical cross-bracings can also be found in the Y direction.

Several process vessels e.g. heat exchanger, surge drum and steam generator are supported on the steel structure and are considered in the modelling. Also, there is a piping network that connects the vessels at different heights. Pipes have three different nominal diameters (DN), viz DN250 40S, DN500 and DN600 80S. More information about the geometrical properties of pipes can be found in [26]. The pipes are made of steel API 5L X42 with expected yielding (f_{yep}) and ultimate strength (f_{uep}) equal to 297.00 MPa and 335.50 MPa, respectively. The modulus of elasticity (E) and Poisson ratio are equal to 203 GPa and 0.2, respectively. Anew, kinematic hardening is considered with rupture strain at 0.03. The piping is supported on the steel structure mainly with sliding and guided supports, so that pipes are free two move in the longitudinal direction; however, some fixed points are also used particularly at the connection of pipes with equipment at the base floor. The description of supports at different coordinates of the system is omitted for brevity.

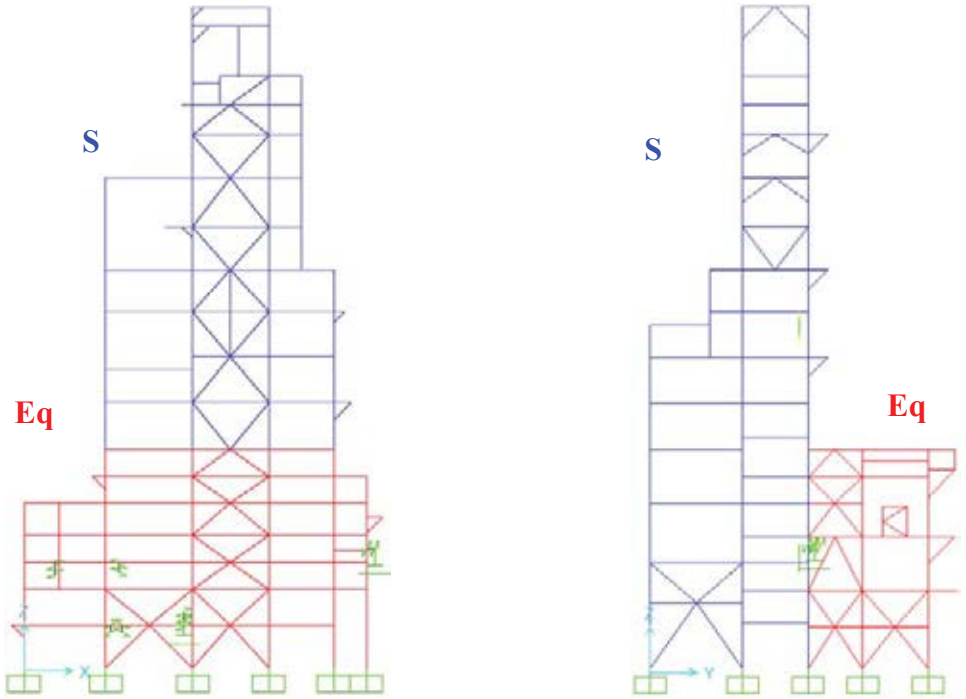

Figure 2: X-Z plane with part S (structure and vertical vessel) and Y-Z plane with part S and Eq (equipment)

Table 1: Impact of panel zone modelling on the first vibration period

Modal Analysis	Panel Zone	T(sec)	ΔT(%)	Mx/My (%)
X-direction	Centerline	1.084	N.A.	32/7
	Rigid offset	1.115	+2.95	22/18
	Scissor	1.073	-1.01	34/5
Y-direction	Centerline	1.175	N.A.	7/32
	Rigid offset	1.048	-10.71	18/22
	Scissor	1.172	-0.20	7/34

N.A.: Not Available

Before considering the assessment of the system in the nonlinear range using [27], it was necessary to examine a number of modelling aspects. First, three different configurations of panel zone were considered to examine the effects on vibration period of the structure, namely centerline without rigid offset, centerline with offset and scissor model as described in [28]. It can be seen in Table 1 that the maximum reduction of period between the centerline (most flexible) and rigid offset configuration was estimated roughly at 11% in the Y direction, whereas the difference with the scissor model did not exceed 3% in both directions. Furthermore, to examine the influence of flexibility of the beam-to-column connections, mainly in the X direction, two different lateral resisting systems were calibrated. In addition to the original system, a dual system was modelled with both directions being restricted. After comparing the vibration modes for the two different structural types, it was concluded that the maximum difference was 8% and 2% in the X direction and Y direction, respectively. Given that the rigid panel zone and the flexibility of connection did not influence considerably the response, the scissor model with the original configuration of frames was considered in the assessment. Finally, Table 2 quotes the first four vibration periods of the entire system, as inferred from modal analysis.

Table 2: The first four modes of vibration of the system

	Mode #	T(sec)	Mx/My (%)
Structural Part S	Mode 1	1.175	32/7
	Mode 2	1.084	7/32
Structural Part E	Mode 3	0.495	30/0
	Mode 4	0.450	0/17

The plastic deformation of structural members was described by concentrated hinge modelling. Although distributed plasticity formulations may capture the stress-strain behaviour along the structural member or local behaviour such as buckling of flanges, they require high computational effort, which becomes even more prohibitive for large scale models like the process unit under examination. On the other hand, point hinges can be more adequate to capturing the nonlinear degrading response [28]. In the framework of this study, concentrated plasticity was used, allowing for an analysis that is both time efficient and effective, under the condition that the response of the system is not investigated beyond the collapse prevention limit state. Concerning the plastic deformation on pipes, fiber sections with 8 integration points were used. More information about this method can be found in [27] and [28].

3.2 Selection of records

The selection of a sufficient number of records for seismic risk assessment is crucial for the accurate prediction of the system response. This comes as a function of the analysis method for deriving fragility functions. For example, the cloud analysis method that the present study employs requires a sufficient number of records with values close to, or larger than, the limit state of interest [29]. Additionally, the method for selecting a set of records consistent with the seismic hazard is equally important for improving the sufficiency and efficiency of the IMs. To this effect, a number of 40 far-field records from NGA West 2 database were selected with the conditional spectrum approach as described by [30]. The spectra of the selected records are shown in Figure 3. The moment magnitude of records, M_w, varies from 6 to 7.6, the Joyner-Boore distance, R_{jb}, spans from 22 to 92 km, approximately. Shorter distance was not considered to avoid including pulse-like records, which are being investigated by the Authors. Also, the average shear wave velocity of the upper 30 m of soil profile, V_{s30}, was found in the range

of 160 km to 360 km which refers to soil type D according to [31]. The records were shortened using the 5-95% significant duration rule and the maximum scale factor was set to 4. Finally, it should be emphasized that the records were conditioned at the first vibration period of the steel structure, T_1, in the weakest direction Y. This decision was made on the basis of the significant inter-storey drift ratio observed at the point where the vertical vessel is supported at the top of the steel structure. Additionally, [32] showed that risk-based assessments do not vary based on the choice of conditioning period given that hazard consistency is achieved.

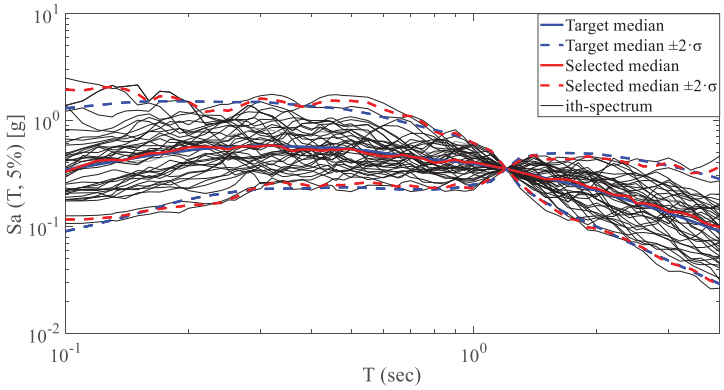

Figure 3: Response spectra of the selected far-field records

4 SEISMIC RISK ASSESSMENT

4.1 Methodology for nonlinear analysis

Before running nonlinear analyses, the acceptance criteria should be defined. There are three main aspects that need to be accounted for when defining performance levels for irregular systems like the process unit. Firstly, the structural type should be considered. The unit is a concentrically braced frame in the X direction and ordinary moment frame with some bracing in the Y direction as well. Also, it lacks diaphragmatic behaviour, which can result in uneven deformation at the same height. Thus, acceptance criteria should not be the same as for common building structures considering also the higher risk that process plants pose to humans and environment. Secondly, the scale of the model necessitates the use of an engineering parameter that is able to describe the damage at global level and can be monitored easily. The shear or moment force of beams and columns as well as the axial force of braces can be suitable parameters for models with smaller scale. Finally, the selected parameter should be able to describe the damage to pipes. For the aforementioned reasons, the interstorey drift ratio (IDR) was selected as a global and generally recognized demand parameter by seismic codes ([24]) to describe the damage on the steel structure. The acceptance criteria for IDR are shown in Table 3 for two different limit states, namely serviceability (SLS) and safe life (SLLS) limit state. [33] investigated the seismic response of a 4-storey steel moment frame analytically and experimentally, indicating that the beginning of yielding and buckling of members occurs at IDR values equal to 1% and 2%, respectively. Given the higher risk, the presence of bracing and irregularity of the process unit, lower values that those indicated by [33] were set for the SLS and SLLS in Table 3. When it comes to piping, the yielding strain is commonly selected as the lower boundary of SLS both under tension and compression. More information about the limit states of piping can be found in [34] and [35].

Furthermore, preliminary time-history analyses were conducted using 11 unscaled records that examined the seismic response of the structure and defined the scaling factor that is required to equal or to exceed the SLLS, which was set as a performance objective. For the cloud

analysis method, there is a rule of thumb saying that 30% of selected records should exceed the desired limit state ([29]). To attain this goal, the records were initially scaled with a scaling factor that did not exceed 5, and then the factor was scaled down to reduce the bias due to some significant deformation that was observed both on steel structure and pipes.

4.2 Efficiency and sufficiency of tested seismic IMs

The scope of the present study is to find an IM that is sufficient and efficient both for the structure and pipes, and which can be combined with a simple ground prediction model for risk assessment. Considering that the system includes structural and nonstructural components and the deficiency of the literature on the seismic response of petrochemical plants units, it was decided to compare measures of three different categories, namely duration-, amplitude- and period response-based. The first category consisted of Arias Intensity (AI, [36]) cumulative and standardized cumulative average velocity (CAV and SCAV, [28]&[29]) and the second one included the peak ground acceleration and velocity (PGA and PGV). Apart from the spectral acceleration at the first vibration period of both structural parts, Sa(T_s) and Sa(T_{Eq}), the effective peak acceleration (EPA, [39]) and the recently introduced equipment average spectral acceleration (E-ASA_R, [19]) were also considered in the period response-based category.

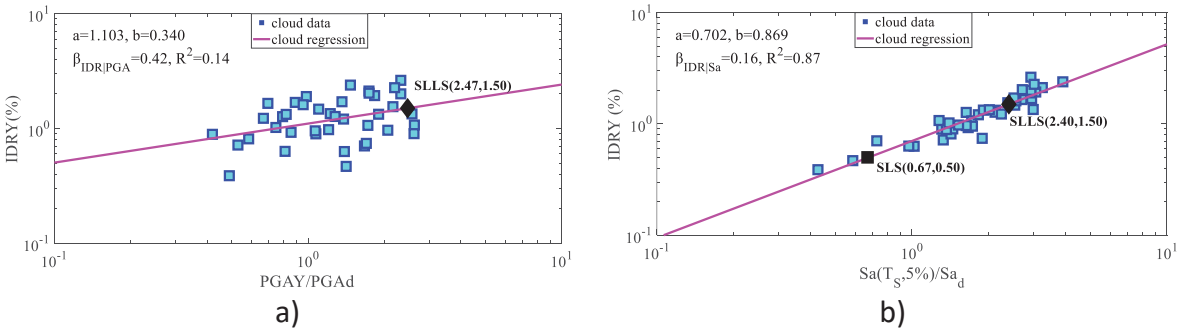

Figure 4: Regression for structural part S using a. PGA in the Y direction, and b. 5%-damped Sa (design values PGA_d and Sa_d are equal to 0.37g and 0.35g, respectively)

Table 3: Median, dispersion and coefficient of determination for structural part S and SLLS

Intensity measure (IM)		$\mu_{lnEDP\|IM}$	$\beta_{EDP\|IM}$	R^2
Duration-based	AIy (m/s)	22.77	0.43	0.10
	CAVy(g-s)	3.57	0.40	0.22
Amplitude-based	PGAy/PGA_d	2.47	0.42	0.14
	PGVy (cm/s)	104.90	0.34	0.44
Period response-based	EPAy (g-s)	0.81	0.29	0.60
	Sa(T_S)/Sa_d	**2.40**	**0.16**	**0.87**

The results from the linear regression analysis of IDR as a function of PGA and Sa for the structural part S in the Y direction are shown in Figure 4a&b, respectively. The most remarkable outcome regards the considerably lower dispersion of Sa compared to the PGA. This outcome stems from the fact that the concentrated mass of the vertical vessel at the top governs the response, resulting in the highest IDR at the same height. The low variability of the response is strengthened further by conditioning the records at the first fundamental mode that pertains mainly to the vibration of the vertical vessel. Obviously, the PGA that is proposed by HAZUS [9] is not efficient and should not be preferred over Sa for risk assessment of this process unit. Also, the rest of IMs were observed to be less efficient than Sa (Table 4). It is emphasized that

Table 4 quotes only the dispersion due to record-to-record randomness. The rest two types of uncertainty are not included to avoid blurring the comparison.

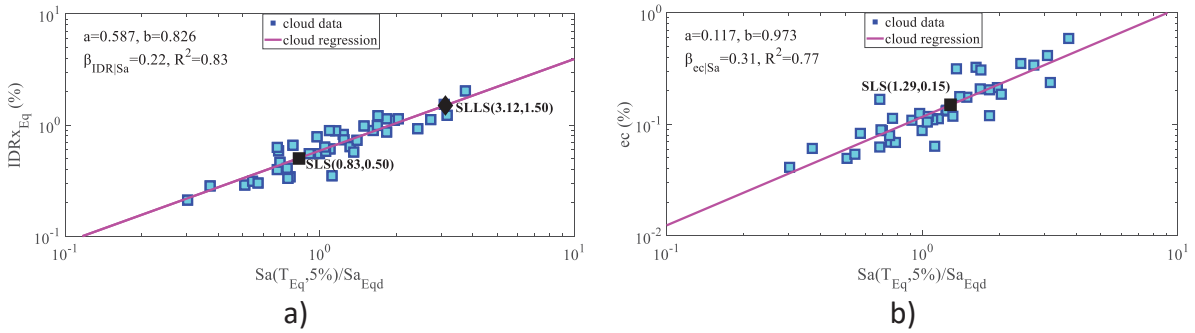

Figure 5: Regression for structural part Eq in terms of a. IDR of steel structure in the X direction and b. compression strain on pipe expressed as a function of 5%-damped Sa_{Eq} (design value, Sa_{Eqd}, equal to 0.94g)

Table 4: Median, dispersion and coefficient of determination for structural part Eq

Intensity measure (IM)		$\mu_{lnEDP\|IM}$	$\beta_{EDP\|IM}$	R^2
Duration-based	AIx (m/s)	6.48	0.54	0.31
	SCAVx (g-s)	1.85	0.59	0.15
Amplitude-based	PGAx/PGA_d	1.48	0.36	0.69
	PGVx (cm/s)	118.90	0.63	0.05
Period response-based	E-ASA40x (g)	0.94	0.35	0.71
	EPAx (g-s)	0.75	0.44	0.53
	$Sa(T_{Eq})/Sa_{Eqd}$|ec	**1.29**	**0.31**	**0.77**
	$Sa(T_{Eq})/Sa_{Eqd}$|IDR	**3.12**	**0.22**	**0.83**

Furthermore, the regression for the structural part Eq, which refers to the steel structure outfitted by the horizontal vessels and pipes, is expressed in terms of interstorey drift, IDR_{Eq}, and pipe strain due to compression, ec, as a function of spectral acceleration at the fundamental frequency of the equipment, $Sa(T_{Eq})$ (mode 3 in Table 2). In this respect, see Figure 5a&b. It can be seen that the SLS for the structure occurred at 36% lower Sa compared to pipes. Additionally, the dispersion for the seismic response of the structure was lower than the pipe, which can be a clear indication that the vulnerability of the equipment should better be expressed in terms of steel structure deformation. It is reasonable that the response of pipes resulted in higher dispersion, since the dynamic interaction of structure, vessel and pipe can become complex, if the pipe is not rigidly supported on the rack. The rest of IMs that were examined resulted in higher dispersion than the above-mentioned measures (Table 5). It is emphasized herein that in contrast with [19] who formulated ESA_R (R means the percentage increase of vibration period) based on the fundamental period of a structure, in this case study, the fundamental period of the structure, $Sa(T_S)$, is much greater than the period of equipment, $Sa(T_{Eq})$, and thus it was decided to use the latter as a reference period and increase it by 40% in order to account for additional modes of vibration of equipment (not shown in Table 2). Nevertheless, it appeared that higher modes apart from T_{Eq} did not affect the response of equipment. Other researchers such as [20] have proposed similar IMs, which do not apply to our case due to the high irregularity of the process unit.

Furthermore, the dependency of IMs on magnitude, M, and Joyner-Boore distance, Rjb, was examined based on the p-value. A p-value greater than 0.05 is commonly accepted as a threshold for accepting the null hypothesis which states that the coefficient of regression is zero. As depicted in Table 6, some measures are sufficient for both parameters and others only for one

of them. It is emphasized that the Sa(T_S) proved to be sufficient for both seismological parameters, thus it meets the requirements to be used for risk assessment in the following. Even though the Sa(T_{Eq}) was sufficient as a function of IDR, it was not evaluated as sufficient with respect to pipe strain, εc (Table 7). Nevertheless, the dispersion of Sa(T_{Eq})|IDR is both efficient and sufficient, and thus it can be used as a proper IM for the risk assessment of the equipment. Finally, the PGA was also a sufficient IM, but lower efficiency was estimated compared to Sa(T_{Eq}).

Table 5: Sufficiency of intensity measures considered for structural part S

Intensity measure (steel structure)		p-value	
		M	Log(Rjb)
Duration-based	AIy	0.0094	0.9673
	CAVy	0.2536	0.3713
Amplitude-based	PGAy/PGA_d	0.0029	0.5643
	PGVy	0.1638	0.5775
Period response-based	EPAy	0.0706	0.6480
	Sa(T_S)/Sa_d	**0.7095**	**0.4879**

Table 6: Sufficiency of intensity measures considered for structural part Eq

Intensity measure (equipment)		p-value	
		M	Log(Rjb)
Duration-based	AIx	0.0585	0.2069
	SCAVx	0.0514	0.0997
Amplitude-based	PGAx/PGA_d	0.6947	0.5745
	PGVx	0.1601	0.0267
Period response-based	E-ASA40x	0.0884	0.1912
	EPAx	0.1631	0.3594
	Sa(T_{Eq})/Sa_{Eqd}|ec	**0.0373**	**0.2231**
	Sa(T_{Eq})/Sa_{Eqd}|IDR	**0.4369**	**0.5460**

4.3 Risk estimation

Based on the previous results, the fragility of the system was derived using the Sa as IM for both structural parts (Figure 6a&b). Also, for the structural part Eq, the fragility for the SLS of the most vulnerable pipe was depicted as well in Figure 6b for the sake of comparison. To derive the mean annual frequency of exceedance for each LS, λ, the fragility curves where integrated with the seismic hazard curves for both parts (Figure 7a&b). The hazard curve provides the mean annual frequency of exceedance, MAF, for each value of Sa. The values of λ for the SLS and SLLS are quoted in Table 8. For the part S, it can be seen that λ is equal to 0.0021 yrs^{-1} or, in other words, the mean return period of exceedance of the SLS is 476 years. Concerning the SLLS and structural part Eq, the mean return period is significantly higher. Based on the fragility analysis results, it can be mentioned that the performance objective of "control damage" on the structure, as stipulated in [24], is met; however, the estimated risk should further be assessed accounting for a greater number of records and soil deformability effects. In such case, the risk can be communicated to a stakeholder for further decision making.

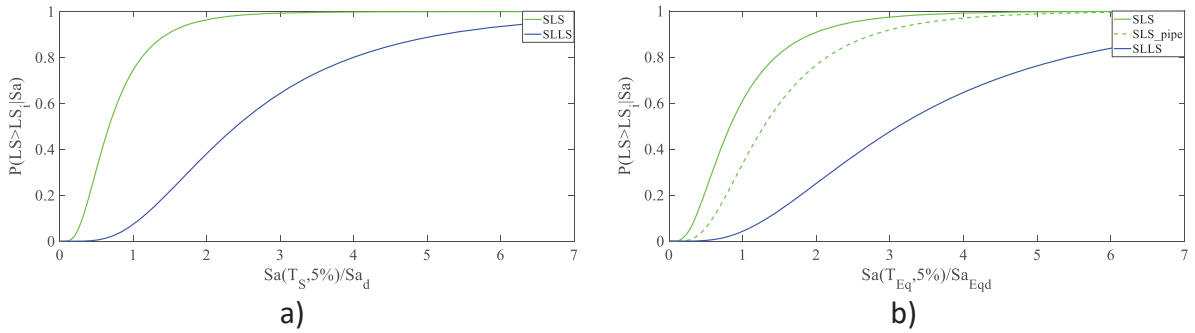

Figure 6: Fragility curves for the a. structural part S and b. structural part Eq

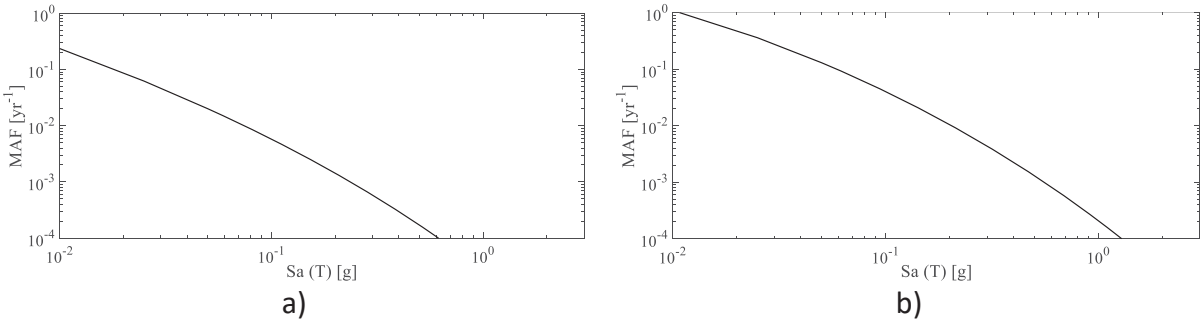

Figure 7: Hazard curves for the a. structural part S and b. structural part Eq

Table 7: Annual frequency of exceedance and return period for the two limit states and structural parts

	PART S		PART Eq	
	λ (yrs^{-1})	Return period (yrs)	λ (yrs^{-1})	Return period (yrs)
SLS	0.0021	476	0.0014	716
SLLS	$1.32 \cdot 10^{-4}$	7,576	$4.67 \cdot 10^{-5}$	21,426

CONCLUSIONS

The present analytical study evaluated the seismic risk of a chemical process unit accounting for dynamic interaction with equipment. The main considerations and outcomes can be summarized as follows:

- The system was separated into two different structural parts, part S and Eq. The part S included the high-rise steel structure, affected mainly by a heavy vertical vessel at the top, whilst the part Eq consisted of the low-rise steel structure and horizontal vessels. This separation was necessary, since the two parts exhibited considerably different vibration periods and the second part included the most vulnerable pipe;
- Using a set of far-field records, the steel structure was found to be more vulnerable than the piping network in both parts, S and Eq. This is because of the excessive concentrated mass of vessels that increased the deformation of steel members;
- Different IMs were considered. However, for both structural parts, S and Eq, the spectral acceleration, was evaluated as both the most efficient and sufficient IM to describe the seismic demand both on the steel structure and piping, although considering a different vibration period for each part.. This outcome brings into question the application of average spectral acceleration, as proposed in the literature, for chemical process units with numerous equipment.

- Finally, the seismic risk was derived for each part separately, and the mean period of exceedance was evaluated at 556 and 1011 years for the SLS. However, the soil deformability should also be considered to have a fully realistic estimation of global risk of the petrochemical plant facility.

Apart from far-field seismic motions, a near-field set of records will be used in the future to examine the seismic vulnerability of the system, accounting for soil-structure interaction. In the end, the results from the fragility analysis will be used for determining consequence scenarios.

ACKNOWLEDGMENTS

The first Author would like to thank Dr. E. Krausmann and Dr. A. Necci for the valuable comments and assistance during the traineeship at Joint Research Center, Ispra. The Authors would like to thank Prof. Carlo G. Lai and Dr. F. Bozzoni from EUCENTRE, Pavia (Italy) for providing the hazard curves for the site under consideration. Finally, the first Author gratefully acknowledges the financial support from the European Commission during the traineeship at the Joint Research Center.

REFERENCES

[1] C. Theofili and A. L. V. Arellano, "Lessons learnt from earthquake disasters that occured in Greece, NEDIES project, EUR 19946 EN," *Jt. Res. Center, Eur. Comm.*, 2001.

[2] M. Eli, S. Sommer, T. Roche, and K. Merz, "The January 17,1994 Northridge Earthquake: Effects on Selected Industrial Facilities and Lifelines," 1995.

[3] E. Krausmann, A. M. Cruz, and B. Affeltranger, "The impact of the 12 May 2008 Wenchuan earthquake on industrial facilities," *J. Loss Prev. Process Ind.*, vol. 23, no. 2, pp. 242–248, 2010.

[4] E. Krausmann, A. M. Cruz, and E. Salzano, *Natech Risk Assessment and Management: Reducing the Risk of Natural-Hazard Impact on Hazardous Installations*. 2016.

[5] M. Campedel, "Analysis of Major Industrial Accidents Triggered by Natural Events Reported In the Principal Available Chemical Accident Databases," 2008.

[6] E. Salzano, I. Iervolino, and G. Fabbrocino, "Seismic risk of atmospheric storage tanks in the framework of quantitative risk analysis," *J. Loss Prev. Process Ind.*, 2003.

[7] A. S. Elnashai and L. Di Sarno, *Fundamentals of Earthquake Engineering: From Source to Fragility*, Second. Wiley, 2015.

[8] A. Necci, E. Krausmann, and S. Girgin, "Emergency planning and response for Natech accidents," *Towar. an All-Hazards Approach to Emerg. Prep. Response Lessons Learn. from Non-Nuclear Events*, 2018.

[9] HAZUS-MH MR5, "Multi-hazard Loss Estimation Methodology Earthquake Model," 2010.

[10] F. T. Kyriazis Pitilakis and K. Kakderi, *Systemic Seismic Vulnerability and Risk Analysis for Buildings, Lifeline Networks and Infrastructures Safety Gain*. 2013.

[11] R. J. Merino Vela, E. Brunesi, and R. Nascimbene, "Seismic assessment of an industrial frame-tank system: development of fragility functions," *Bull. Earthq. Eng.*, vol. 17, no. 5, pp. 2569–2602, May 2019.

[12] O. S. Bursi, F. Paolacci, and S. Reza, "Performance-Based Analysis Of Coupled Support Structures And Piping Systems Subject To Seismic Loading," *ASME 2015 Press. Vessel. Pip. Conf.*, vol. 00032, no. July 2015, pp. 1–8.

[13] O. S. Bursi and M. S. et al Reza, "Component Fragility Evaluation, Seismic Safety Assessment and Design of Petrochemical Plants under Design-basis and Beyond-design-basis Accident Conditions. Mid-Term Report, INDUSE-2-SAFETY Project, Contr. No: RFS-PR-13056, Research Fund for Coal and Ste," 2019.

[14] Y. S. Salem, P. E. Tiffany Yoo, G. M. Gad, and J. S. Cho, "Analytical Fragility Curves for Pipe Rack Structure," 2019, pp. 292–306.

[15] N. Luco and C. A. Cornell, "Structure-specific scalar intensity measures for near-source and ordinary earthquake ground motions," *Earthq. Spectra*, 2007.

[16] G. Tsinidis, L. Di Sarno, A. Sextos, and P. Furtner, "Optimal intensity measures for the structural assessment of buried steel natural gas pipelines due to seismically-induced axial compression at geotechnical discontinuities," *Soil Dyn. Earthq. Eng.*, 2020.

[17] J. E. Padgett, B. G. Nielson, and R. DesRoches, "Selection of optimal intensity measures in probabilistic seismic demand models of highway bridge portfolios," *Earthq. Eng. Struct. Dyn.*, 2008.

[18] R. Maio and G. Tsionis, "Seismic fragility curves for the European building stock: Review and evaluation of analytical fragility curves," 2016.

[19] M. De Biasio, S. Grange, F. Dufour, F. Allain, and I. Petre-Lazar, "Intensity measures for probabilistic assessment of non-structural components acceleration demand," *Earthq. Eng. Struct. Dyn.*, vol. 44, no. 13, pp. 2261–2280, Oct. 2015.

[20] M. Kohrangi, P. Bazzurro, D. Vamvatsikos, and A. Spillatura, "Conditional spectrum-based ground motion record selection using average spectral acceleration," *Earthq. Eng. Struct. Dyn.*, 2017.

[21] C. A. Cornell, F. Jalayer, R. O. Hamburger, and D. A. Foutch, "Probabilistic Basis for 2000 SAC Federal Emergency Management Agency Steel Moment Frame Guidelines," *J. Struct. Eng.*, 2002.

[22] I. C. Council, *2018 International Building Code*. 2018.

[23] F. Bozzoni *et al.*, "Probabilistic seismic hazard assessment at the eastern Caribbean Islands," *Bull. Seismol. Soc. Am.*, 2011.

[24] ASCE/SEI 41-17, *Seismic Evaluation and Retrofit of Existing Buildings*. American Society of Civil Engineers, 2017.

[25] R. Pekelnicky and C. Poland, "ASCE 41-13: Seismic Evaluation and Retrofit Rehabilitation of Existing Buildings," *SEAOC 2012 Conv. Proc.*, 2012.

[26] *ASME B36.19M-2004 Stainless steel pipe (Revision of ANSI/ASME B36.19M-1985), American national standard*. .

[27] CSI, "SAP2000. Analysis Reference Manual v.18.1.1," *CSI: Berkeley (CA, USA): Computers and Structures INC*. p. 496, 2018.

[28] ATC 114, "Recommended modeling parameters and acceptance criteria for nonlinear analysis in support of seismic evaluation, retrofit, and design," *Nist Gcr 17-917-45*, 2017.

[29] F. Jalayer, H. Ebrahimian, A. Miano, G. Manfredi, and H. Sezen, "Analytical fragility assessment using unscaled ground motion records," *Earthq. Eng. Struct. Dyn.*, 2017.

[30] J. W. Baker and C. Lee, "An Improved Algorithm for Selecting Ground Motions to Match a Conditional Spectrum," *J. Earthq. Eng.*, 2018.

[31] ASCE/SEI 7-16, *Minimum Design Loads and Associated Criteria for Buildings and Other Structures*. 2017.

[32] T. Lin, C. B. Haselton, and J. W. Baker, "Conditional spectrum-based ground motion selection. Part I: Hazard consistency for risk-based assessments," *Earthq. Eng. Struct. Dyn.*, 2013.

[33] K. Suita, S. Yamada, M. Tada, K. Kasai, Y. Matsuoka, and Y. Shimada, "Collapse experiment on 4-story steel moment frame: part 2 detail of collapse behavior," *Proc. 14th world Conf. Earthq. Eng. Beijing, China*, 2008.

[34] L. Di Sarno and G. Karagiannakis, "On the seismic fragility of pipe rack—piping systems considering soil–structure interaction," *Bull. Earthq. Eng.*, Feb. 2020.

[35] M. Vathi, S. A. Karamanos, I. A. Kapogiannis, and K. V. Spiliopoulos, "Performance criteria for liquid storage tanks and piping systems subjected to seismic loading," *J. Press. Vessel Technol.*, 2017.

[36] A. Arias, "A measure of earthquake intensity. Seismic Design for Nuclear Power Plants," in *Seismic Design for Nuclear Power Plants*, 1970.

[37] J. W. Reed and R. P. Kassawara, "A criterion for determining exceedance of the operating basis earthquake," *Nucl. Eng. Des.*, 1990.

[38] EPRI, "Standardization of the cumulative absolute velocity. EPRI TR-100082. Electric Power Research Institute, USA," 1991.

[39] ATC, "Tentative provisions for the development of seismic regulations for buildings, ATC-3-06 Report, Applied Technology Council, Redwood City, CA.," 1978.